

## THE OPTICAL DEPTH OF THE 158 MICRON [ $^{12}\text{C II}$ ] LINE: DETECTION OF THE $F = 1 \rightarrow 0$ [ $^{13}\text{C II}$ ] HYPERFINE-STRUCTURE COMPONENT

G. J. STACEY,<sup>1</sup> C. H. TOWNES,<sup>1</sup> A. POGLITSCH,<sup>2</sup> S. C. MADDEN,<sup>2</sup> J. M. JACKSON,<sup>3</sup> F. HERRMANN,<sup>2</sup>  
 R. GENZEL,<sup>2</sup> AND N. GEIS<sup>4</sup>

Received 1990 December 26; accepted 1991 September 5

### ABSTRACT

We report the first detection of the  $F = 1 \rightarrow 0$  hyperfine component of the 158  $\mu\text{m}$  [ $^{13}\text{C II}$ ] fine-structure line in the interstellar medium. A 12 point intensity map was obtained of the [ $^{13}\text{C II}$ ] distribution over the inner  $190''$  (R.A.)  $\times$   $190''$  (decl.) regions of the Orion Nebula using an imaging Fabry-Perot interferometer. The [ $^{12}\text{C II}$ ]/[ $^{13}\text{C II}$ ] line intensity ratio varies significantly over the region mapped. It is highest ( $86 \pm 9$ ) in the core of the Orion H II region, and significantly lower ( $62 \pm 7$ ) in the outer regions of the map, reflecting higher optical depth in the [ $^{12}\text{C II}$ ] line here. We suggest that this enhanced optical depth is the result of limb brightening of the optically thin [ $^{13}\text{C II}$ ] line at the edges of the bowl-shaped H II region blister. If the  $^{12}\text{C}/^{13}\text{C}$  abundance ratio is 43, the [ $^{12}\text{C II}$ ] line in the inner regions of the Orion Nebula has a low optical depth:  $\tau_{12} \sim 0.75 \pm 0.25$ . The optical depth together with the large brightness temperature of the [ $^{12}\text{C II}$ ] line ( $\sim 160$  K) requires that the excitation temperature of the  $^2P_{3/2}$  level be  $\sim 310$  K, in very good agreement with the previous analysis of the physical conditions of the Orion interface region based on fine-structure line intensity ratios and photodissociation region models. If the  $^{12}\text{C}/^{13}\text{C}$  abundance ratio is 67, the line optical depth is somewhat larger ( $\tau_{12} \sim 1.85$ ), and the transition excitation temperature is somewhat smaller ( $\sim 190$  K) than that predicted by these models. The present results therefore support values  $\sim 43$  for the  $^{12}\text{C}/^{13}\text{C}$  abundance ratio in the Orion Nebula.

*Subject headings:* infrared: spectra — interstellar: matter — nebulae: Orion Nebula

### 1. INTRODUCTION

The  $^2P_{3/2} \rightarrow ^2P_{1/2}$  fine-structure transition of singly ionized carbon is among the brightest emission lines from Galactic star formation regions and may be the single brightest emission line from external galaxies (cf. Crawford et al. 1985 and Stacey et al. 1991b and references therein). Much of the [C II] line radiation from both the Galaxy and external galaxies arises in the warm ( $T_{\text{gas}} \gtrsim 200$  K), dense ( $n_{\text{H}} \gtrsim 10^3 \text{ cm}^{-3}$ ) photodissociated gas regions found on the surfaces of giant molecular clouds exposed to the ionizing far-ultraviolet (FUV) radiation of nearby early-type stars or the general FUV interstellar radiation field. The gas in these “photodissociation” regions (PDRs) is heated through both the photoelectric ejection of energetic electrons from grains and the collisional de-excitation of UV-pumped vibrationally excited  $\text{H}_2$  molecules, and cooled mainly through the fine-structure line radiation of  $\text{C}^+$ ,  $\text{O}^0$ , and  $\text{Si}^+$  (cf. Tielens & Hollenbach 1985a and Sternberg & Dalgarno 1989). Due to its proximity, the Orion H II region/molecular cloud interface region has been the primary laboratory for the study of photodissociation regions. Radiative transfer studies of the [O I] and [C II] line intensity ratios have indicated that the Orion PDR has gas kinetic temperatures,  $T_{\text{gas}} \sim 250 \rightarrow 350$  K, gas densities,  $n_{\text{H}} \sim 2 \rightarrow 4 \times 10^5 \text{ cm}^{-3}$ , and  $\text{C}^+$  column densities,  $N_{\text{C}^+} \sim 3 \rightarrow 5 \times 10^{18} \text{ cm}^{-2}$  with line center optical depth of the [ $^{12}\text{C II}$ ] line,  $\tau_{12} \sim 0.5 \rightarrow 1$

(Stacey et al. 1983; Stacey 1985; Crawford et al. 1985; Stacey et al. 1991c). Tielens & Hollenbach (1985b) constructed a photodissociation region model of the Orion interface region, which includes gas chemistry, UV radiation field strength, and thermal balance as a function of depth into the molecular cloud. This model reproduces most of the important far-infrared fine-structure line intensities observed from the Orion interface region with similar physical parameters for the emitting gas:  $N_{\text{C}^+} \sim 3 \rightarrow 5 \times 10^{18} \text{ cm}^{-2}$ ,  $n_{\text{H}} \sim 1 \rightarrow 2 \times 10^5 \text{ cm}^{-3}$ ,  $265 < T_{\text{gas}} < 500$  K;  $\tau_{12} \lesssim 1$  (see also Wolfire, Tielens, & Hollenbach 1990). However, Boreiko, Betz, & Zmuidzinas (1988) reported detection of the  $F = 2 \rightarrow 1$  hyperfine component of the 158  $\mu\text{m}$  [ $^{13}\text{C II}$ ] fine-structure line from  $\Theta^1$  Ori C and BN-KL at intensity levels consistent with optically thick ( $\tau_{12} \sim 5 \rightarrow 6$ ) emission in the  $^{12}\text{C}^+$  fine-structure line (assumed  $^{12}\text{C}/^{13}\text{C}$  abundance ratio  $\sim 60$ ). This high optical depth requires that the gas temperatures are 2–3 times lower and column densities 2–3 times greater than previous estimates (Tielens & Hollenbach 1985b). The surprising disparity between these results and the previous observational and theoretical work prompted the new observations reported here.

Since the  $^{13}\text{C}$  nucleus has nuclear spin  $I = \frac{1}{2}$ , the fine-structure levels  $J$  are split into hyperfine structure levels depending on the value of the quantum number  $F = J \pm I$ . The  $F = 2 \rightarrow 0$  component is highly forbidden; therefore, the  $^2P_{3/2} \rightarrow ^2P_{1/2}$  fine structure line of [ $^{13}\text{C II}$ ] is effectively split into just three components:  $F = 2 \rightarrow 1$ ,  $F = 1 \rightarrow 1$ , and  $F = 1 \rightarrow 0$ . The corresponding [ $^{12}\text{C II}$ ] line is not split since the nuclear spin of  $^{12}\text{C}$  is zero. Cooksy, Blake, & Saykally (1986) have determined the transition frequencies of the [ $^{12}\text{C II}$ ] and [ $^{13}\text{C II}$ ] fine-structure transitions to high precision using laser magnetic resonance spectroscopy. In velocity space, the  $F = 1 \rightarrow 0$ ,  $2 \rightarrow 1$ , and  $1 \rightarrow 1$  components of [ $^{13}\text{C II}$ ] occur at  $-65.2 (\pm 2.4)$ ,  $+11.2 (\pm 0.36)$ , and  $+63.2 (\pm 1.6)$  km

<sup>1</sup> Department of Physics, University of California, Berkeley, Berkeley, CA 94720.

<sup>2</sup> Max-Planck-Institut für Physik und Astrophysik, Institut für extraterrestrische Physik, D-8046 Garching bei München, Germany.

<sup>3</sup> Department of Astronomy, Boston University, 725 Commonwealth Avenue, Boston, MA 02215.

<sup>4</sup> Max-Planck-Institut für extraterrestrische Physik, Garching. Present address: Department of Physics, University of California, Berkeley, Berkeley, CA 94720.

$s^{-1}$  with respect to the  $[^{12}\text{C II}]$  transition at 1900.5369 GHz (157.7409  $\mu\text{m}$ ). The relative line intensity ratios in optically thin, thermalized gas ( $n_{\text{H}} \gg n_{\text{crit}} \sim 3 \times 10^3 \text{ cm}^{-3}$ ) are 35.6%, 44.4%, and 20.0%, respectively.

## 2. OBSERVATIONS

The  $[\text{C II}]$  line observations were obtained with the MPE/UCB Far-infrared Imaging Fabry-Perot Interferometer (FIFI; Poglitsch et al. 1991, Geis 1991) during a flight on the Kuiper Airborne Observatory (KAO) on the night of 1990 September 29. Our observations employed a square  $5 \times 5$  array of stressed Ge:Ga photoconductors (Stacey et al. 1991a) with a  $40''$  separation between adjacent pixels. We employed a spectral resolution of  $3 \times 10^4$  ( $10 \text{ km s}^{-1}$ ) for the pixel which is on the optical axis (ideally the central pixel) of the scanning Fabry-Perot. Pixels off the optical axis of the Fabry-Perot have somewhat reduced spectral resolution due to the angular divergence of the beam in the scanning Fabry-Perot, which substantially reduces the utility of the outer elements of the array at the high spectral resolutions employed here (Poglitsch et al. 1991). In addition, the scanning Fabry-Perot transmits at shorter wavelengths for the off-axis pixels, resulting in an apparent redshifting of spectral lines for these pixels. For the discussion which follows, we will refer to pixels in terms of their right ascension–declination offsets in seconds of arc with respect to the central pixel.

The observations were obtained with the central pixel pointed at  $\Theta^1 \text{ Ori C}$  ( $\alpha_{1950} = 5^{\text{h}}32^{\text{m}}49^{\text{s}}.0$ ,  $\delta_{1950} = -5^{\circ}24'16''$ ). The pointing was better than  $10''$  and a rotating “K” mirror maintains the detector array axes in right ascension–declination coordinates during the entire observing leg. The telescope chopper throw was  $6'5 \text{ E-W}$  at a frequency of 23 Hz. Our (approximately Gaussian-shaped) beam with the 91.4 cm telescope on the KAO is  $55''$  for each pixel (FWHM; beam solid angle  $\sim 8.3 \times 10^{-8} \text{ sr}$ ;  $67''$  equivalent disk). The system noise equivalent power, including all losses, ranged between  $\sim 3$  and  $5 \times 10^{-15} \text{ W Hz}^{1/2}$  for the various pixels.

We chose to observe the  $F = 1 \rightarrow 0$  component of  $[^{13}\text{C II}]$  rather than the somewhat brighter  $F = 2 \rightarrow 1$  component because the former component is further removed in velocity space from the bright  $[^{12}\text{C II}]$  line. This ensures good spectral separation between the  $[^{12}\text{C II}]$  and  $[^{13}\text{C II}]$  lines thus precluding the possibility of an incorrect identification of high velocity emission from the  $[^{12}\text{C II}]$  line as the  $[^{13}\text{C II}]$  line. To obtain the best measurement of the  $[^{12}\text{C II}]/[^{13}\text{C II}]$  line intensity ratio, it is important to observe the two lines on the same flight with as close as possible to the same experimental set up thereby minimizing systematic effects. Both lines are easily observable within the same spectral scan with our instrument, but we split this spectral scan into two parts to achieve the highest signal-to-noise ratio for the  $[^{13}\text{C II}]$  line. We first made four  $50 \text{ km s}^{-1}$  (five resolution element) scans centered on the  $[^{12}\text{C II}]$  line with a total integration time of 120 s. Next, we shifted the scan  $65.2 \pm 0.8 \text{ km s}^{-1}$  to the blue of the observed  $[^{12}\text{C II}]$  line to center on the expected position of the  $F = 1 \rightarrow 0$   $[^{13}\text{C II}]$  line. We integrated for 42 minutes here. As before, each scan was five  $10 \text{ km s}^{-1}$  resolution elements wide. The relative spacing of the two scans was verified periodically through broad ( $250 \text{ km s}^{-1}$  wide) scans centered on the  $[^{13}\text{C II}]$  scan center which then also included the bright  $[^{12}\text{C II}]$  line. The instrument-sky coupling factor (0.7; Poglitsch et al. 1991) was verified through continuum measurements of Mars. We estimate the uncertainty in absolute flux

calibration to be less than 30%. Relative calibration between the  $[^{12}\text{C II}]$  and  $[^{13}\text{C II}]$  lines is probably better than 10%.

## 3. RESULTS

The high signal-to-noise ratio achieved on the  $[^{12}\text{C II}]$  line enables us to verify the optical alignment of the scanning Fabry-Perot through pixel-by-pixel inspection of the relative velocity shifts and spectral broadening of the  $[^{12}\text{C II}]$  line. Assuming the  $[^{12}\text{C II}]$  line widths and velocity shifts across the interface region are small with respect to the velocity resolution employed, the most blueshifted pixel (and also the narrowest spectrum) will correspond to the pixel which is best aligned with the optical axis of the scanning Fabry-Perot. Inspection of our  $50 \text{ km s}^{-1}$  scans of the  $[^{12}\text{C II}]$  line verifies that the optical axis is close to the northeast corner of the central ( $0''$ ,  $0''$ ) pixel. Therefore, the 12 highest sensitivity pixels form a cross-shaped pattern centered in the upper half of the  $5 \times 5$  pixel array (see Fig. 2).

### 3.1. Detection of the $[^{13}\text{C II}] F = 1 \rightarrow 0$ Transition

To achieve a highly significant measure of the  $[^{13}\text{C II}]$  line intensity averaged over the inner regions of the Orion nebula, we co-added the  $[^{13}\text{C II}]$  spectra from these 12 pixels. Before the co-addition, each individual spectrum was shifted to match the velocity shifts measured in its corresponding  $[^{12}\text{C II}]$  line. Figure 1 is the concatenation of the average  $[^{13}\text{C II}]$  spectrum thus obtained with the corresponding  $[^{12}\text{C II}]$  spectrum. To fit the observed  $[^{12}\text{C II}]$  profile, we convolved our instrumental profile with a variable width Gaussian curve representing the intrinsic source line profile. The least-squares best fit (*dashed line*) is obtained for an intrinsic  $[^{12}\text{C II}]$  line width of  $\sim 4.6 \pm 0.7 \text{ km s}^{-1}$ , in excellent agreement with the results of Boreiko et al. (1988). The wings of the instrumental profile

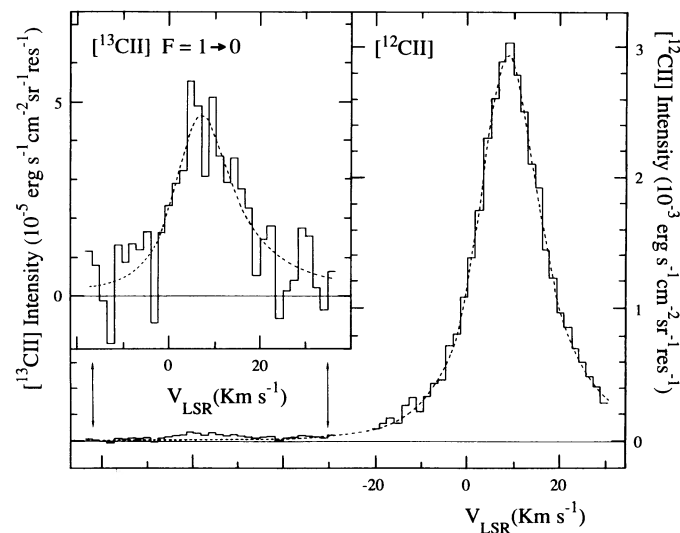


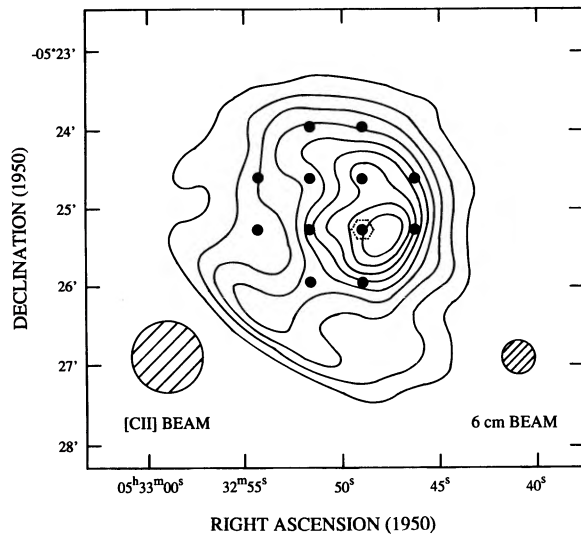
FIG. 1.—Superposed  $[^{12}\text{C II}]$  and  $[^{13}\text{C II}]$  spectra obtained toward the Orion interface region. The  $F = 1 \rightarrow 0$  hyperfine component of  $[^{13}\text{C II}]$  occurs at  $-65.2 \pm 2.4 \text{ km s}^{-1}$  with respect to the  $[^{12}\text{C II}]$  line. The observed  $[^{12}\text{C II}]$  spectrum (*right*) and the  $[^{13}\text{C II}]$  (*left*) each are the co-addition of the 12 central channels of the array. Total integration time was 24 and 504 minutes, respectively. Our instrumental profile is a modified Lorentzian of equivalent width  $\pi/2 \cdot \Delta V_{\text{FWHM}}$ . The spectral resolution averaged over the 12 pixels is  $15 \text{ km s}^{-1}$ . The dashed lines represent best-fit instrumental profiles to the observed spectra. The wing of the  $[^{12}\text{C II}]$  spectrum was removed for the  $[^{13}\text{C II}]$  spectrum shown in the expanded scale (inset).

impose a slightly curved baseline on the [ $^{13}\text{C II}$ ] spectrum. The inset is the [ $^{13}\text{C II}$ ] spectrum with this baseline subtracted and the intensity scale multiplied by 30.

The [ $^{13}\text{C II}$ ] line is clearly detected at an integrated intensity level of  $I_{13} \sim 4.71 \pm 0.24 \times 10^{-5} \text{ ergs s}^{-1} \text{ cm}^{-2} \text{ sr}^{-1}$ , which is 69 times weaker than the [ $^{12}\text{C II}$ ] line ( $I_{12} \sim 3.25 \times 10^{-3} \text{ ergs s}^{-1} \text{ cm}^{-2} \text{ sr}^{-1}$ ). Our best-fit instrumental profile (*dashed line*) indicates an intrinsic line width of  $4.0 \pm 1 \text{ km s}^{-1}$ , similar to the value obtained for the [ $^{12}\text{C II}$ ] line. The line center is  $\sim 1.2 \pm 1.1 \text{ km s}^{-1}$  to the blue with respect to the scan center, indicating a true rest wavelength of the  $F = 1 \rightarrow 0$  transition of  $157.7060 \pm 0.0007 \mu\text{m}$  (1  $\sigma$ ), or  $-66.4 \pm 1.4 \text{ km s}^{-1}$  with respect to the [ $^{12}\text{C II}$ ] line. This new value is in good agreement with the  $F = 1 \rightarrow 0$  rest wavelength [ $157.7066 \pm 0.0013 \mu\text{m}$  (2  $\sigma$ )] given by Cooksy et al. (1986) and may be used for refined estimates of the  $^{13}\text{C}^+$  atomic constants.

### 3.2. Mapping Results

Figure 2 (*left*) indicates the positions of our 12 pixels on the 6 cm radio continuum contours of Johnston et al. (1983) (28" beam). Figure 2 (*right*) lists the observed [ $^{12}\text{C II}$ ] and [ $^{13}\text{C II}$ ] line intensities, line intensity ratios, and inferred [ $^{12}\text{C II}$ ] optical depth (see below) for each position. The [ $^{12}\text{C II}$ ] line distribution is uniform to  $\sim 30\%$  over most of the region mapped. In contrast the 6 cm continuum emission falls by a factor of nearly five between the peak near  $\Theta^1 \text{ Ori C}$  and the outer pixels of our map. This supports the model that the [C II] line radiation originates in the interface region between the H II region and the molecular cloud—not from within the H II region itself. The uniformity of the [ $^{12}\text{C II}$ ] distribution is the result of the weak dependence of the [ $^{12}\text{C II}$ ] line intensity on the incident UV radiation field for radiation fields as high as those found in the Orion interface region ( $\sim 10^5$  times the local interstellar radiation field; cf. Tielens & Hollenbach 1985b).



The [ $^{12}\text{C II}$ ] and [ $^{13}\text{C II}$ ] line intensities in each pixel were obtained with the fitting procedure described above. The [ $^{13}\text{C II}$ ] line is firmly detected ( $\geq 4 \sigma$ ) in 10 of the 12 pixels, and is marginally detected (2.5  $\sigma$ ) in one other. The [ $^{12}\text{C II}$ ]/[ $^{13}\text{C II}$ ] line intensity ratio is not constant over the map. That ratio is highest for the inner four pixels ( $86 \pm 9$ ) and systematically lower over the outer eight pixel regions ( $62 \pm 7$ ). The ratio is especially small for the pixel at  $(-40'', 0'')$ . This change in the line intensity ratio is naturally explained in terms of the geometry of the Orion interface region. The inner four pixels are pointed toward the “core” of the Orion H II region, where the 6 cm radio contours do not change rapidly, and the interface region is viewed nearly face-on. Most of the outer pixels lie on steep gradients in the 6 cm emission, and may therefore represent the edge of the bowl-shaped “blister” at the H II region/molecular cloud interface. Just outside of these pixels there is a sharp gradient in the [ $^{12}\text{C II}$ ] line emission consistent with this scenario (Stacey et al. 1991c). The very optically thin [ $^{13}\text{C II}$ ] emission may be somewhat enhanced with respect to the [ $^{12}\text{C II}$ ] emission at the positions of greater optical depth produced by these nearly edge-on interfaces.

The  $F = 2 \rightarrow 1$  transition is too close in velocity to the [ $^{12}\text{C II}$ ] line to allow an accurate determination of its intensity from the observed [ $^{12}\text{C II}$ ] spectrum. However, our observed [ $^{13}\text{C II}$ ]  $F = 1 \rightarrow 0$  intensity toward  $\Theta^1 \text{ Ori C}$  ( $I_{13} = 4.43 \pm 0.78 \times 10^{-5} \text{ ergs s}^{-1} \text{ cm}^{-2} \text{ sr}^{-1}$ ) would correspond to an intensity of  $5.48 \pm 0.96 \times 10^{-5} \text{ ergs s}^{-1} \text{ cm}^{-2} \text{ sr}^{-1}$  in the  $F = 2 \rightarrow 1$  transition assuming thermodynamic equilibrium between the two lines. This intensity is in agreement (within

FIG. 2.—*Left*: Beam positions for the 12 pixels used in this analysis (*filled circles*) superposed on the 6 cm radio continuum of Johnston et al. (1983) (28" beam). The contour levels are 10, 20, 30, 40, 50, 60, 70, 80, and 90% of the peak flux density ( $4.75 \text{ Jy beam}^{-1}$ ). The [C II] beam (55") is shown in the lower left-hand corner. The central pixel ( $\Theta^1 \text{ Ori C}$ ) is enclosed by a dotted hexagon. *Right*: Measured [ $^{12}\text{C II}$ ] and [ $^{13}\text{C II}$ ] line intensities (*first and second lines*), the line intensity ratio (*third line*), and the [ $^{12}\text{C II}$ ] line optical depth,  $\tau_{12}$  (*fourth line*), distribution over the mapped regions. The [ $^{12}\text{C II}$ ] and [ $^{13}\text{C II}$ ] intensities are obtained through fits of the instrumental profile to each spectrum. The map is not corrected for self-chopping (20% effect). We have assumed a  $^{12}\text{C}/^{13}\text{C}$  abundance ratio of 43 for the optical depth estimates. Error bars represent one standard deviation from the mean.



stated errors) with the value obtained toward  $\Theta^1$  Ori C by Boreiko et al. (1988) [ $I_{13}(F=2 \rightarrow 1) = 7.6 \pm 2.5 \times 10^{-5}$  ergs  $s^{-1} \text{ cm}^{-2} \text{ sr}^{-1}$ ]. The optical depth obtained below, however, is substantially different than that obtained by Boreiko et al., both due to the observed differences in the [ $^{13}\text{C II}$ ] line intensity and differences in estimates of the intrinsic [ $^{13}\text{C II}$ ] line width.

#### 4. DISCUSSION

For the high-UV fields present in the Orion interface region, the penetration of carbon-ionizing photons into the molecular cloud is limited by absorption by dust (cf. Tielens & Hollenbach 1985a). Therefore, we expect that the  $^{13}\text{C}^+$  and  $^{12}\text{C}^+$  columns will be coextensive, and the [ $^{12}\text{C II}$ ]/[ $^{13}\text{C II}$ ] line intensity ratio will depend only on the gas phase carbon abundance and physical conditions of the emitting gas.

##### 4.1. Optical Depth of the [ $^{12}\text{C II}$ ] Line

In the limit of optically thin emission in the [ $^{13}\text{C II}$ ] line, the ratio of the [ $^{12}\text{C II}$ ] to [ $^{13}\text{C II}$ ] line intensities,  $R$ , is given by:

$$R \equiv \frac{I_{12}}{I_{13}} = \left[ \frac{1 - \exp(-\tau_{12})}{1 - \exp(-\tau_{13})} \right] = \frac{^{12}\text{C}/^{13}\text{C}}{f_{i \rightarrow j}} \left[ \frac{1 - \exp(-\tau_{12})}{\tau_{12}} \right],$$

where  $^{12}\text{C}/^{13}\text{C}$  is the ratio of abundances,  $\tau_{12}$  and  $\tau_{13}$  are the optical depths of the [ $^{12}\text{C II}$ ] and [ $^{13}\text{C II}$ ] lines, respectively ( $\tau_{12} = ^{12}\text{C}/^{13}\text{C} \tau_{13}$ ), and  $f_{i \rightarrow j}$  is the fraction of the total [ $^{13}\text{C II}$ ] line intensity which is contained in the  $F = i \rightarrow j$  hyperfine component ( $f_{1 \rightarrow 0} = 0.356$ ).

The line intensity ratio is directly proportional to the assumed abundance ratio. Therefore, the derived optical depth will be very sensitive to the abundance ratio. Figure 2b displays the calculated optical depth of the [ $^{12}\text{C II}$ ] line assuming an isotopic abundance ratio of 43 as obtained by Hawkins & Jura (1987) (see also Johansson et al. 1984). The optical depth of the [ $^{12}\text{C II}$ ] line varies significantly over the mapped region. The smallest optical depths are obtained for the inner regions of the nebula. For the inner four pixel region, the average line intensity ratio ( $86 \pm 9$ ) indicates a [ $^{12}\text{C II}$ ] line optical depth of  $\tau_{12} = 0.75 \pm 0.25$  averaged over our spectral profile. Our measured intrinsic [ $^{13}\text{C II}$ ] and [ $^{12}\text{C II}$ ] line widths would indicate a somewhat higher line center optical depth ( $\sim 1.0$ ). The outer eight pixels show significantly higher optical depth than the inner regions:  $\tau_{12} = 1.5 \pm 0.3$ . If the abundance ratio were as high as 67, as suggested by Langer & Penzias (1990), we obtain an optical depth of  $1.85 \pm 0.3$  for the inner regions and  $2.8 \pm 0.4$  for the outer regions of the nebula. For the high abundance ratios, the optical depth may reach a value as high as  $5.2^{+1.8}_{-1.1}$  at the  $(-40'', 0'')$  pixel.

Support for the low abundance ratio solution is obtained by comparison of the observed line [ $^{12}\text{C II}$ ] and [ $^{13}\text{C II}$ ] line widths. The line width ratio is a function of the optical depth of the two lines. Averaged over the Orion nebula, the [ $^{12}\text{C II}$ ]/[ $^{13}\text{C II}$ ] line intensity ratio is  $69 \pm 5$ , or  $\tau_{12} = 1.25 \pm 0.15$  for an assumed abundance ratio of 43. If this were the optical depth of the [ $^{12}\text{C II}$ ] line, one would expect a ratio of the line widths  $\sim 1.22$  (cf. Phillips et al. 1979). The observed line width

ratio is  $\Delta v([^{12}\text{C II}])/\Delta v([^{13}\text{C II}]) = 1.16 \pm 0.34$ . For an abundance ratio of 67, the line intensity ratio averaged over the Orion Nebula implies  $\tau_{12} = 2.5$  and the predicted line width ratio would be  $\sim 1.45$ .

##### 4.2. Physical Conditions of the Photodissociated Gas

The observed brightness temperature of the [ $^{13}\text{C II}$ ] line together with its optical depth may be used to derive the excitation temperature of the transition. The average intensity of the [ $^{12}\text{C II}$ ] line for the inner four pixels is  $\sim 3.3 \times 10^{-3}$  ergs  $s^{-1} \text{ cm}^{-2} \text{ sr}^{-1}$ . With an observed line width of  $5 \text{ km s}^{-1}$  (Boreiko et al. 1988), we obtain a main-beam Rayleigh-Jeans brightness temperature of  $T_{\text{RJ}} \sim 94 \text{ K}$ , in good agreement with the  $T_{\text{RJ}} \sim 88 \text{ K}$  obtained by Boreiko et al. (1988). The chopper throw available on the KAO precluded chopping to regions on the sky devoid of [C II] line radiation from the Orion molecular cloud (Stacey et al. 1991c). This “self-chopping” was evident during flight: the measured [ $^{12}\text{C II}$ ] line intensity was consistently stronger when the reference beam was to the west than when the reference beam was to the east. The correction for this self-chopping is  $\sim 20\%$  (Stacey et al. 1991c), so that the true intensities and brightness temperatures are  $I_{12} \sim 4.15 \times 10^{-3}$  ergs  $s^{-1} \text{ cm}^{-2} \text{ sr}^{-1}$  and  $T_{\text{RJ}} \sim 120$ , respectively. The Planck-corrected brightness temperature is  $T_p \sim 160 \text{ K}$ . This is the minimum corrected temperature for the emitting medium appropriate in the high density, high optical depth limit. This brightness temperature and the optical depth  $\tau_{12} \sim 0.75 \pm 0.25$  deduced above implies a transition excitation temperature of  $260 \lesssim T_{\text{ex}} \lesssim 410 \text{ K}$  with a most likely value of  $310 \text{ K}$ . Since the emitting medium has densities  $\gtrsim 10^5 \text{ cm}^{-3}$ , which is much in excess of the critical density for the transition, this excitation temperature is a very good indicator of the true gas kinetic temperature. The column density of  $^{12}\text{C}^+$  ions along the line of sight is  $N_{\text{C}^+} \sim 4.1 \times 10^{18} \text{ cm}^{-2}$  for these excitation conditions and our observed [ $^{13}\text{C II}$ ] line intensity (Crawford et al. 1985). Assuming  $\text{C}^+/\text{H} = 3 \times 10^{-4}$  this corresponds to a column density of hydrogen nuclei of  $\sim 1.4 \times 10^{22} \text{ cm}^{-2}$ , or a visual extinction of 7. These physical parameters derived for the [C II]-emitting photodissociated gas are in very good agreement with the values obtained in the photodissociation region models (Tielens & Hollenbach 1985b; Wolfire, et al. 1990) and those derived from the observed [O I] and [C II] line intensity ratios (Stacey et al. 1983; Stacey 1985; Crawford et al. 1985; Stacey et al. 1991c):  $T_{\text{gas}} \sim 250 \rightarrow 350 \text{ K}$ ;  $\tau_{12} \sim 0.5 \rightarrow 1$ ,  $N_{\text{C}^+} \sim 3 \rightarrow 5 \times 10^{18} \text{ cm}^{-2}$ . If the abundance ratio,  $^{12}\text{C}/^{13}\text{C}$  were 67, then the agreement is not as good. For this abundance ratio,  $\tau_{12} \sim 1.85$  so that  $T_{\text{gas}} \sim 190 \text{ K}$  and  $N_{\text{C}^+} \sim 6.9 \times 10^{18} \text{ cm}^{-2}$ . The present results therefore favor the lower values for the  $^{12}\text{C}/^{13}\text{C}$  abundance ratio.

We thank the staff and crew of the Kuiper Airborne Observatory for their excellent support. We also thank A. I. Harris for critical readings of a previous draft, J. B. Lugten for useful discussions, and an anonymous referee for important criticism of a previous draft. This work was supported by NASA grant NAG2-208.

#### REFERENCES

- Boreiko, R. T., Betz, A. L., & Zmuidzinas, J. 1988, ApJ, 325, L47  
 Cooks, A. S., Blake, G. A., & Saykally, R. J. 1986, ApJ, 305, L89  
 Crawford, M. K., Genzel, R., Townes, C. H., & Watson, D. M. 1985, ApJ, 291, 755  
 Geis, N. 1991, Ph.D. thesis, Ludwig-Maximilians-University, Munich  
 Hawkins, I., & Jura, M. 1987, ApJ, 317, 926  
 Johansson, L. E. B., et al. 1984, A&A, 130, 227  
 Johnston, K. J., Palmer, P., Wilson, T. L., & Bieging, J. H. 1983, ApJ 271, L89  
 Langer, W. D., & Penzias, A. A. 1990, ApJ, 357, 477  
 Phillips, T. G., Huggins, P. J., Wannier, P. G., & Scoville, N. Z. 1979, ApJ, 231,

720

Poglitsch, A., et al. 1991, Int. J. Infrared Millimeter Waves, in press

Stacey, G. J. 1985, Ph.D. thesis, Cornell University

Stacey, G. J., Beaman, J., Geis, N., Haller, E. E., Poglitsch, A., &amp; Rumitz, M.

1991a, in preparation

Stacey, G. J., Geis, N., Genzel, R., Lugten, J. B., Poglitsch, A., Sternberg, A., &amp;

Townes, C. H. 1991b, ApJ, 373, 423

Stacey, G. J., Genzel, R., Harris, A. I., Jaffe, D. T., Poglitsch, A., Stutzki, J., &amp;

Townes, C. H. 1991c, in preparation

Stacey, G. J., Smyers, S. D., Kurtz, N. T., &amp; Harwit, M. 1983, ApJ, 265, L7

Sternberg, A., &amp; Dalgarno, A. 1989, ApJ, 338, 197

Tielens, A. G. G. M., &amp; Hollenbach, D. 1985a, ApJ, 291, 722

———. 1985b, ApJ, 291, 747

Wolfire, M. G., Tielens, A. G. G. M., &amp; Hollenbach, D. 1990, ApJ, 358, 116